Pers Ubiquit Comput (2018) 22:275–287
DOI 10.1007/s00779-017-1042-0

ORIGINAL ARTICLE

SVM-based classification method to identify alcohol consumption using ECG and PPG monitoring

Wen-Fong Wang[1] · Ching-Yu Yang[2] · Yan-Fu Wu[1]

Received: 29 November 2016 / Accepted: 19 May 2017 / Published online: 28 June 2017

Abstract Driving under the influence (DUI) of alcohol ("drunk driving") is dangerous and may cause serious harm to people and damage to property. To address this problem, this study developed a system for identifying excess alcohol consumption. Electrocardiogram (ECG) and photoplethysmography (PPG) sensors and intoxilyzers were used to acquire signals regarding the ECG, PPG, and alcohol consumption levels of participants before and after drinking. The signals were preprocessed, segmented, and subjected to feature extraction using specific algorithms to produce ECG and PPG training and test data. Based on the ECG, PPG, and alcohol consumption data we developed a fast and accurate identification scheme using the support vector machine (SVM) algorithm for identifying alcohol consumption. Optimized SVM classifiers were trained using the training data, and the test data were applied to verify the identification performance of the trained SVMs. The identification performance of the proposed classifiers achieved 95% on average. In this study, different feature combinations were tested to select the optimum technological configuration. Because the PPG and ECG features produce identical classification performance and the PPG features are more convenient to acquire, the technological configuration based on PPG is definitely preferable for developing smart and wearable devices for the identification of DUI.

Keywords Alcohol · Wearable · SVM · ECG · PPG

✉ Wen-Fong Wang
wwf@yuntech.edu.tw

Ching-Yu Yang
chingyu@npu.edu.tw

Yan-Fu Wu
m10217033@yuntech.edu.tw

[1] Department of CSIE, National Yunlin University of Science & Technology, Douliu, Yunlin, 640 Taiwan

[2] Department of CSIE, National Penghu University of Science & Technology, Makung, Penghu, 880 Taiwan

1 Introduction

Driving under the influence (DUI), or driving while intoxicated, is a criminal offense that involves driving a motor vehicle after consuming alcohol to a level that renders the driver incapable of operating the motor vehicle safely [1]. Current national criteria for identifying DUI rely on breath alcohol concentration (BrAC) tests, which are measured in milligrams per liter, or blood alcohol concentration (BAC) tests, which are measured in grams per deciliter [2, 3]. Being DUI a major factor in traffic accidents, many appeals have been made to governments to realize more stringent implementations of preventative measures and DUI laws [4].

In an early study on the effect of alcohol on humans [5], the researchers divided the subjects into two groups, namely normal and alcohol dependence. Using 24-h recording, the study recorded the differences in heart rate (HR) and heart rate variability (HRV) for the two groups. The researchers found that the alcohol dependence group exhibited greater variations in HR and HRV and also had a higher risk of cardiovascular disease. In [6], healthy subjects were recruited and divided into two categories, namely juice drinking and alcohol drinking, to observe the differences in changes in R-R intervals (RRIs) over time. The results showed that the RRI of the subjects in the alcohol drinking category was time-varying and inconsistent. In [7], participants were requested to consume a fixed amount of alcohol per week.

After long-term observation and analysis, the researchers concluded that alcohol consumption is highly correlated with HR and HRV variations. In [8], the recruited participants were young and free of cardiovascular diseases and alcohol and drug addiction. Using analysis of electrocardiogram (ECG) variations, the researchers observed the cardiac autonomic regulation of the participants after alcohol consumption. HR was found to follow changes in blood alcohol content. According to the aforementioned research, ECG is affected significantly by alcohol intake.

ECG signals are produced by the changes in voltage (membrane potential) during heartbeats and are an important means of observing the activities of cardiac systole and diastole. ECG signals not only correspond to the condition of the heart but can also be used as an indicator of physiological or psychological change. Recently, extensive studies of ECG have been conducted. For example, significant changes in ECG signals were observed because of altitude and low temperature [9–12]. Studies have been conducted on HR variations before and after exercise, and the ECG variations have been applied to train classifiers for emotional perception identification [13–15]. Sleep status has also been examined through changes in ECG and respiratory signals [16].

Photoplethysmography (PPG) is an optical technique for the detection of volumetric changes in microvascular blood flow in the fingers or skin [17]. A PPG sensor may consist of a light-emitting diode light source and a photodetector, which produces voltage signals proportional to the quantity of peripheral blood flow at the measuring point. The voltage variations from PPG sensors are closely related to HR and ECG readings [17]. Because PPG provides valuable information related to cardiovascular systems and is a noninvasive method in which measurements are made at the skin surface, it is suitable for DUI identification. Hence, this study attempted to apply ECG and PPG to establish effective signal features for recognizing alcohol consumption.

In [18], the authors identified three approaches to detecting DUI, namely direct detection through blood alcohol testing, behavior-based detection, and biosignal-based detection. The first two approaches are insufficient to meet requirements of simultaneous early warning, full automation, and high accuracy. However, the biosignal-based detection can meet all of these requirements. Therefore, the authors proposed weighted kernel-based support vector machine (SVM) classifiers based on ECG signals for identifying alcohol consumption. In addition, they acquired ECG signals from normal and intoxicated subjects and extracted 10 ECG features related to alcohol metabolism in the human body for the identification of alcohol consumption.

For practical application, the intoxilyzers used in BrAC tests are expensive and unsuitable to be worn or installed in motor vehicles [19]. The purpose of this study is to develop a quick and easy scheme for more effectively identifying the degree to which drivers are intoxicated after consuming alcohol. The proposed scheme is based on detecting physiological signals using ECG and PPG.

The rest of this paper is organized as follows. In Section 2, the physiological signals used are described, and the signal noise and characteristics are defined. In Section 3, the steps involved in processing the ECG and PPG signals are explained in detail, including signal preprocessing, segmentation, feature extraction, and classification. Section 4 presents the experimental results. Finally, some concluding remarks are presented in the last section.

2 Materials

2.1 Signal acquisition

For physiological signal acquisition, a PowerLab 8/30 data acquisition system was employed to record digital ECG and PPG signals. The system comprises three parts: an ECG signal amplifier [20], a PPG signal amplifier [21], and a data acquisition system [22]. Because the ECG and PPG signals acquired from the front-end device are too weak to process, the signals must be amplified before signal processing. Therefore, they are processed by the amplifiers and then transmitted to the data acquisition system for the production of digitized ECG and PPG signals.

In the ECG signal acquisition process, the measurement method was based on standard limb lead 1 configuration that entails affixing electrodes to a participant's limbs [23]. Three ECG sensor electrodes were employed, with one positive electrode attached on the left arm, one negative electrode attached to the right arm, and one grounded electrode affixed to the participant's right ankle. For the PPG signal acquisition, a clip style sensor front-end was used, and the forefinger of the subject was held in the clip for measurement. Because the sensors are susceptible to interference as the signals are being acquired, participants were asked to remain as still as possible. In the data acquisition phase, participants sat while the experiment was conducted. To prevent excessive and unnecessary noise, they were asked to minimize their limb movement. In addition, the data acquisition system was used to synchronize the digitized ECG and PPG signals for producing other parameters for DUI classification.

2.2 Physiological signals and noise

Regarding the ECG measurement, twelve leads can be used. For convenient measurement of ECG signals, standard limb lead 1 configuration was used in this study. As shown in Fig. 1a, a complete cardiac cycle (which is a complex wave)

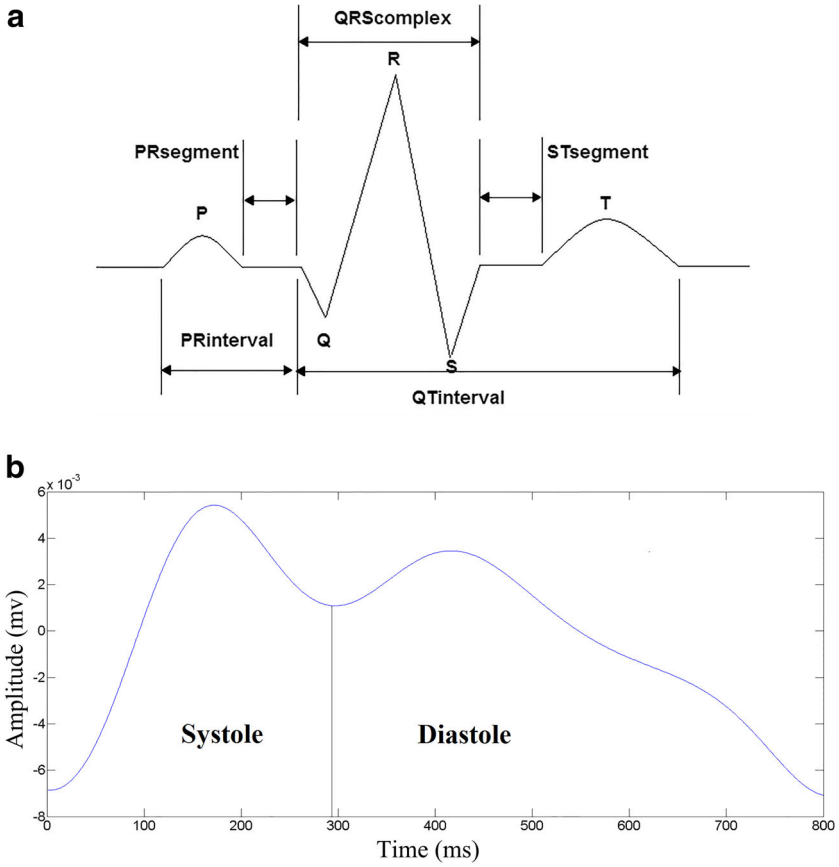

Fig. 1 Complete cardiac cycle: **a** ECG and **b** PPG

measured from the standard limb lead 1 comprises a P wave, a QRS wave, and a T wave, corresponding to atrial contraction, ventricular contraction, and ventricular diastole, respectively. Because the R peak of the QRS wave is the most obvious feature point in ECG signals, it was marked as a feature for segmenting the cardiac cycles in this study.

As shown in Fig. 1b, PPG signals are composed of systolic and diastolic phases due to heartbeats and cyclical changes in intravascular blood flow. The signals of systolic and diastolic blood pressure can be found in a complete PPG waveform.

During the ECG recording process, noise from external environmental interference may be mixed with actual signals and can interfere with signal analysis. Therefore, the noise must be preemptively identified and removed. The types of noise presented by Friesen et al. [24] are listed in Table 1. ECG high-frequency and baseline wander noise can significantly degrade the original signals. According to the spectrum of the aforementioned noise, digital filters such as a Butterworth filter can be used to remove the noise [25]. Regarding PPG noise, external factors can also cause the data acquisition system to receive many non-PPG signals. The types of PPG noise, which were suggested by Lee et al. [26], are listed in Table 1. A digital filter can also be applied to remove such noise.

2.3 Experimental procedure

The sobriety tests of this study were conducted in a clean and quiet laboratory in order to minimize interference from outside sources. Participants were requested to blow into an intoxilyzer (Fig. 2) to enable their BrAC to be determined [19]. In [27], the author indicated that numerous factors influence the degree to which alcohol is absorbed and distributed throughout the body. Higher levels of alcohol consumption result in higher BAC and BrAC levels being detected, and at such levels, individuals become more dangerous while operating vehicles. However, no global standard DUI identification criteria based on BAC and

Table 1 ECG and PPG noises and their associated frequency

Types of interferences	Frequency (Hz)
ECG power interference	60
ECG electrode contact noise	60
ECG instrument noise	100 ∼ 1000
ECG muscle contraction	DC ∼ 10000
ECG baseline wander	0.15 ∼ 0.3
PPG baseline wander	0.04 ∼ 1.6
PPG motion artifact	0 or higher

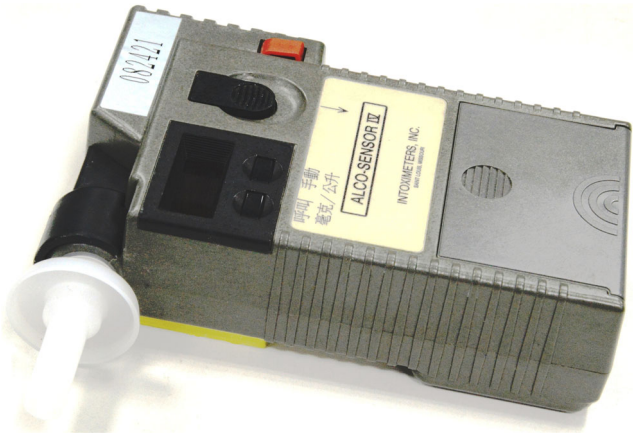

Fig. 2 Intoxilyzer

BrAC have been established. A very strict BAC limit for driving set at 0.03 g/dL (or 0.15 mg/L at BrAC) is reported in [27], and this was employed as a basis for the classification of alcohol consumption for the tests in the current study.

In [28], the BAC and BrAC test results were shown to be highly and positively correlated. The ratio of BrAC to BAC is approximately 1:2100 [29]. For example, 0.2 mg/L in BrAC can be converted approximately to 0.04 g/dL in BAC. Based on BAC, the primary amount of alcohol consumption under testing (ACtest; mL) can be obtained for each participant before testing.

$$ACtest = \frac{0.7 \times BW \times BAC}{ABV \times D}, \tag{1}$$

where 0.7 is the Widmark's coefficient [30], BW is the body weight (kg), ABV is the alcohol content (%), and D is the density (g/mL). The calculation of the drinking volume derived from (1) was implemented based on a BAC of 0.04 g/dL. This level of alcohol consumption can result in detected BrACs that can vary from 0 to in excess of 0.15 mg/L.

Due to the extra preparation time for each test after drinking, the alcohol metabolism of the human body and the duration under its influence should be considered. Notably, the efficiency with which alcohol is metabolized varies among people. To test the effective dose of alcohol in the systemic circulation, a suitable quantity must be determined for one specific participant. The ethanol metabolism rate of the human body is approximately 0.1 g/Kg/h under normal conditions [29]. Thus, the formula for the alcohol metabolism (AlcMetab; mL) of the human body can be calculated as follows:

$$AlcMetab = \frac{0.1 \times BW \times Hr}{ABV \times D}, \tag{2}$$

where Hr is the elapsed time from the beginning of drinking (h). Combined with ACtest (1) and AlcMetab (2), the sufficient dose of drinking alcohol (SufDose; mL) for the tests is defined below:

$$SufDose = ACtest + AlcMetab. \tag{3}$$

For the selection of subjects, young male participants were mainly selected, with the criteria that they were not heavy drinkers and had no history of cardiovascular problems. Therefore, the participants were first asked to complete the Cut, Annoyed, Guilty, and Eye-opener (CAGE) scale to assess their compliance [31]. They were then divided into two categories, namely **cat_A** for drinking "all in one go" and **cat_B** for gradual incremental drinking.

In the tests, the participants drank neat 40% whiskey in the morning after an overnight fast. For **cat_A**, the participants consumed the whiskey in one go. A complete flow diagram of the test procedure is depicted in Fig. 3a. For **cat_B**, the participants consumed the whiskey in gradual increments according to the test procedure shown in Fig. 3b. The participants adopted a sitting posture to complete the experiment. The necessary quantity of neat whiskey to be consumed was determined using (1)–(3). The same participants conducted the **cat_A** and **cat_B** experiments at separate times.

Figure 3 provides flow diagrams of the test procedures, which consisted of six steps. The first step involved acquiring ECG and PPG signals before the sobriety test (Step 1). Due to alcohol remaining in the mouth, the BrAC detected by an intoxilyzer can diverge considerably from the actual BrAC if alcohol detection is conducted immediately after drinking. To avoid inaccurate BrAC detection, the participants were requested to wait for 15 min. before blowing into the intoxilyzer. In the **cat_A** test procedure, the participants were requested to rest after drinking the quantity of whiskey (determined according to (3)) that caused their BAC to be 0.04 g/dL (Step 2a). In the **cat_B** test procedure, four test runs were conducted in which the participants were requested to rest after drinking the determined quantity of whiskey (by (3)) that increased their BAC by 0.01 g/dL per test run (Step 2b).

After resting for 15 min., their BrAC values were measured using the intoxilyzer and then recorded (Step 3). Immediately after the sobriety test, their ECG and PPG signals were measured for 3 min. to set up the physiological data record (Step 4). In each test run, an extra rest took place for the subsequent 7 min. (Step 5).

For **cat_A**, the test procedure iterated Steps 3, 4, 5, and 6a, with each run lasting for 10 min. The test procedure continued until the result of the sobriety test was zero (Step 6a). For **cat_B**, the test procedure iterated Steps 2b, 3, 4, 5, and 6b, with each run lasting for 25 min. The procedure ends when the participant has drunk the fourth dose. (Step 6b).

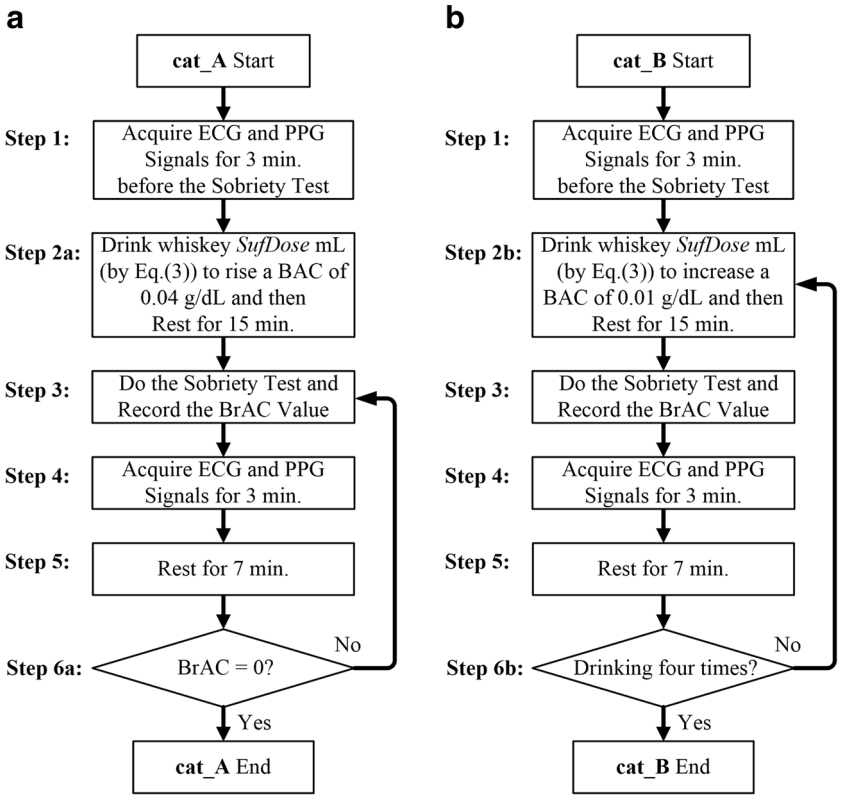

Fig. 3 Flow diagrams of the alcohol test procedures for **a cat_A** and **b cat_B**

2.4 Definition of heartbeat characteristics

In [32], the authors observed that excessive alcohol consumption, in the absence of organic heart disease, may produce changes in ECG signals, and that the predominate abnormalities were sinus tachycardia and nonspecific T-wave changes. In [18], the authors found that the prominent variations in the ECG characteristics between the signals for normal and intoxicated participants were changes in the peak values, RRIs, and P wave duration. These findings demonstrate that the R peak value and RRI are relatively significant characteristics that can be detected by wearable ECG/PPG sensors. Other characteristics are less easy to acquire because of the requirement for multiple ECG leads; that is, achieving effective and reliable measurement using the sensors is highly inconvenient for the wearer. Table 2 lists the selected ECG and PPG characteristics necessary for realizing the identification of alcohol consumption in wearable devices; these are considered to be the prominent features of the variation in BAC and BrAC and the easiest to classify if the subjects have consumed alcohol.

In Fig. 4, R_i indicates a maximum signal magnitude caused by the ventricular contraction in a heartbeat. Because it is a prominent identification position in ECG signals, R_i is appropriate for application in segmenting ECG signals for each heartbeat and is also used as a feature together with $\overline{R}_i$ and R_sd_i for the identification. The RRI is defined as the length of a time interval between any two successive R peaks (see RRI_i in Table 2), essentially corresponding to a cardiac cycle. Because RRI_i is very vulnerable to—and easily affected by—the changes in the external environment and internal psychological factors, it is well-suited for use as a feature for classifying alcohol consumption. HRV can be measured by calculating RRI_sd_i (the standard deviation of RRI_i, as indicated in Table 2). It is well known that several factors, including alcohol, may increase the irregularity of heartbeats, thus $\overline{RRI}_i$ and RRI_sd_i were selected as input features for classification.

In [33], the authors observed that PPG signals were closely related to blood pressure, with PPG waves closely agreeing with the curve of arterial pressure during one cardiac cycle. Regarding the PPG wave of a cardiac cycle, $PPGsys_i$ (Fig. 4), $\overline{PPGsys}_i$, and $PPGsys\_sd_i$ were selected as features for the identification of alcohol consumption. Corresponding to RRI_i, $\overline{RRI}_i$, and RRI_sd_i, PPI_i, which is the time interval between two successive $PPGsys_i$, $\overline{PPI}_i$, and its standard deviation PPI_sd_i were also applied as features.

$PPGsys_i$ appears later than R_i within a cardiac cycle. This time difference is termed the pulse transmission time (PTT), as shown in Fig. 4. Because HR and HRV are sensitive to variations in alcohol concentration [5], and the PTT is closely related to the ventricular systole and its associated arterial pulse in one cardiac cycle, PTT_i, $\overline{PTT}_i$,

Table 2 Selected characteristics in ECG and PPG signals

Characteristics	Definition
R_i	The peak value of the QRS wave in the ith heartbeat
$\overline{R_i}$	The mean of R_i from the first to ith heartbeats
R_sd_i	The standard deviation (sd) of R_i from the first to ith heartbeats
RRI_i	The time interval between R_i and R_{i+1}
$\overline{RRI}_i$	The mean of RRI_i till the $(i+1)$th heartbeat
RRI_sd_i	The standard deviation of RRI_i
$PPGsys_i$	The peak value of the PPG systole wave in the ith heartbeat
$\overline{PPGsys}_i$	The mean of $PPGsys_i$ from the first to ith heartbeats
$PPGsys\_sd_i$	The standard deviation of $PPGsys_i$
PPI_i	The time interval between $PPGsys_i$ and $PPGsys_{i+1}$
$\overline{PPI}_i$	The mean of PPI_i till the $(i+1)$th heartbeat
PPI_sd_i	The standard deviation of PPI_i
PTT_i	The time interval between $PPGsys_i$ and R_i
$\overline{PTT}_i$	The mean of PTT_i till the ith heartbeat
PTT_sd_i	The standard deviation of PTT_i
$cov(R_i, \quad PTT\_sd_i)$	The covariance of R_i and PTT_sd_i
$cov(PPGsys_i, \quad PTT\_sd_i)$	The covariance of $PPGsys_i$ and PTT_sd_i

and PTT_sd_i are proposed as features to facilitate the classification of alcohol consumption in this study. In addition, the covariances of PTT_sd_i with R_i and $PPGsys_i$ are proposed as features because the variation in PTT_i could be closely related to the signal magnitudes of R_i and $PPGsys_i$.

3 Methods

The main elements of the signal processing procedure are shown in Fig. 5. In particular, after being acquired, the signal is preprocessed and segmented. Then, features are extracted and given as input to the classifiers. The signals were preprocessed to remove the noise from the original ECG and PPG signals after the spectrum analysis by using fast Fourier transform (FFT). In the signal segmentation process, a proposed algorithm based on modulus-maxima wavelet (MMW) analysis was devised to identify the features R_i and $PPGsys_i$. Each cardiac cycle could be delineated based on the two features [34, 35]. In the feature extraction process, other features (Table 2) could be computed through the delineated cardiac cycles. For classification, the distinct combinations of the aforementioned features were constructed. The feature combinations were then given as input to the SVMs to identify the extent of intoxication circumstances of the participants.

3.1 Signal preprocessing

In signal preprocessing, noise, including electrical noise and baseline wander from respiration, was identified and filtered

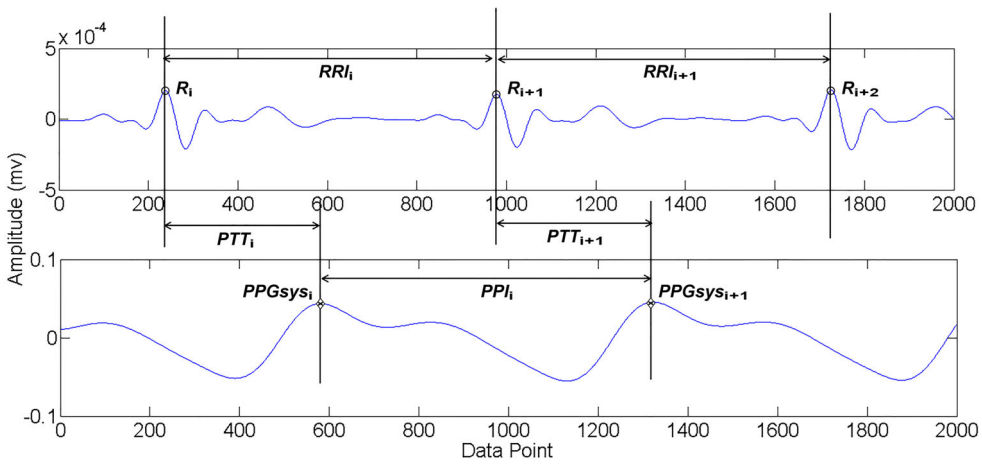

Fig. 4 Synchronized ECG and PPG signals in successive heartbeats

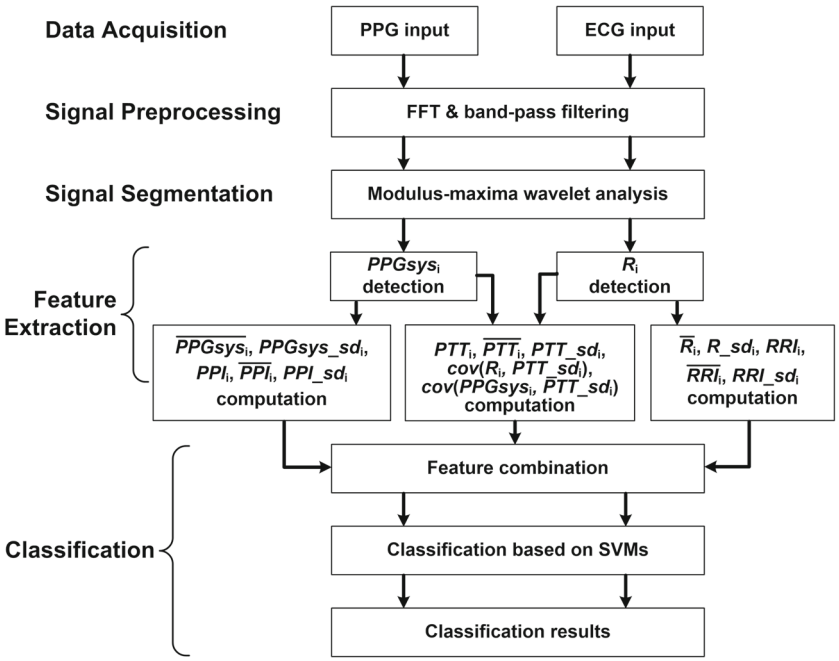

Fig. 5 Flow diagram of signal processing

from original signals. To remove noise, the original signals are first analysed via FFT to observe their energy distribution (Fig. 6). This is done to identify the noise band in ECG and PPG signals. The bandwidth distribution of ECG and PPG signals processed by FFT are illustrated in Fig. 6. The baseline wander noise in the ECG and PPG signals and the power interference in ECG are clearly marked. The major signal bands for ECG and PPG were observed to be from 4 to 20 Hz and 1 to 4 Hz, respectively (Fig. 6). The cause of this noise interference is that the signal acquisition was performed with the participants in a sitting posture. Therefore, no motion artifacts were produced by body movements or

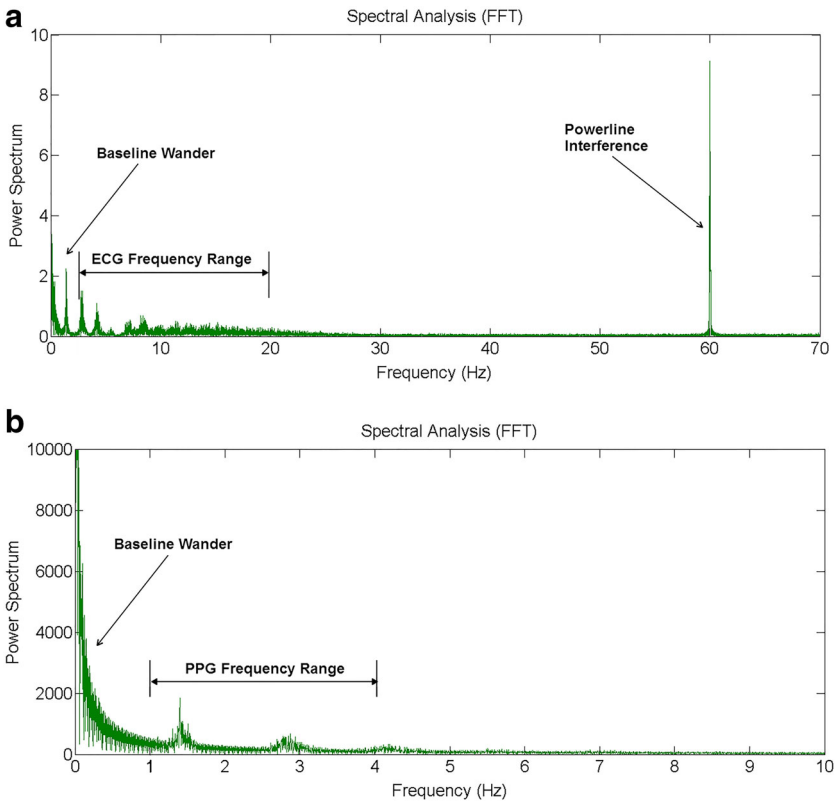

Fig. 6 FFT spectral analysis of the signal and noise bands: **a** ECG and **b** PPG

physical contact. With the exception of the aforementioned ECG and PPG signal bands, the remaining signals could be treated as noise and removed from the original signals.

After the FFT spectral analysis, we applied a Kaiser window-based digital FIR filter, which has desirable properties in both the time and frequency domains, for processing ECG signals [36]. This can effectively filter noise and retain the original ECG and PPG signals. In this study, the sampling frequency of data acquisition was set to 1000 Hz, which can fit the effective sampling rate required by the ECG and PPG acquisition for identifying alcohol consumption. Because the Kaiser filter was applied for bandpass filtering in this study, the low and high cutoff frequencies for ECG were set to 4 and 20 Hz, respectively. The filtering results are shown in Fig. 7a. For PPG, the low and high cutoff frequencies were set to 1 and 4 Hz, respectively; the processing result is shown in Fig. 7b.

3.2 Signal segmentation and feature extraction

The purpose of signal segmentation was to identify single cardiac cycles in the filtered ECG and PPG signals. For a single cycle, R_i and $PPGsys_i$ were extracted first, and subsequently, the rest of the features in Table 2 were extracted for the classification of alcohol consumption. Let SIG_{filt} be the set of the filtered ECG and PPG signals, where $SIG_{filt} = \{(i, x(i))|\, x(i)$ is the sampled ECG or PPG value, $1 \leq i \leq N\}$, i is a timing index corresponding to signal sampling, and N is the number of samples.

To identify each cardiac cycle, a cardiac cycle segmentation algorithm (which includes MMW to analyze SIG_{filt}) was devised to extract signal extrema from SIG_{filt} [35]. The algorithm was then applied to determine the sets of ECG and PPG positive signal peaks (which were represented by the sets ECG_Peak and PPG_Peak for all R_i and $PPGsys_i$, respectively) from the signal extrema produced by MMW. However, it was still necessary for the distance between any two successive peaks in ECG_Peak and PPG_Peak to be validated to assure the accuracy of the extracted cardiac cycles in the ECG and PPG signals. To validate the marking correctness of R_i and $PPGsys_i$ and compute the remaining features, a cardiac cycle validation and feature computation algorithm was devised. In [37], four rules are provided for validating cardiac cycles implemented using the aforementioned algorithm. If the distance between any two successive peaks in ECG_Peak and PPG_Peak were invalid after the validation, the distance between the two peaks would be treated as zero, and the two peaks were ignored. Following validation, the remaining features in Table 2 were calculated by the algorithm.

3.3 Feature combination and classification

After extracting the features from the ECG and PPG signals, we organized them into two groups (ECG and PPG) with eight combinations, as listed in Table 3. The feature combinations were used to classify alcohol consumption and compare the efficiency of the extracted features in the classification. Because acquiring cardiological signals using ECG and PPG differs markedly regarding convenience, the classification efficiency of the feature combinations can reveal the technological advantage of applying either ECG or PPG for smart and wearable devices.

To construct an SVM model for classifying the degree of intoxication of participants, let w be a decision hyperplane normal vector, $\{x_1, \cdots, x_n\}$ be the data set, and $y_i \in \{1, -1\}$ be the class label for each x_i. Then, the SVM classifier can be formed using (4).

$$f(x_i) = sign(w^T \cdot x_i + b), \tag{4}$$

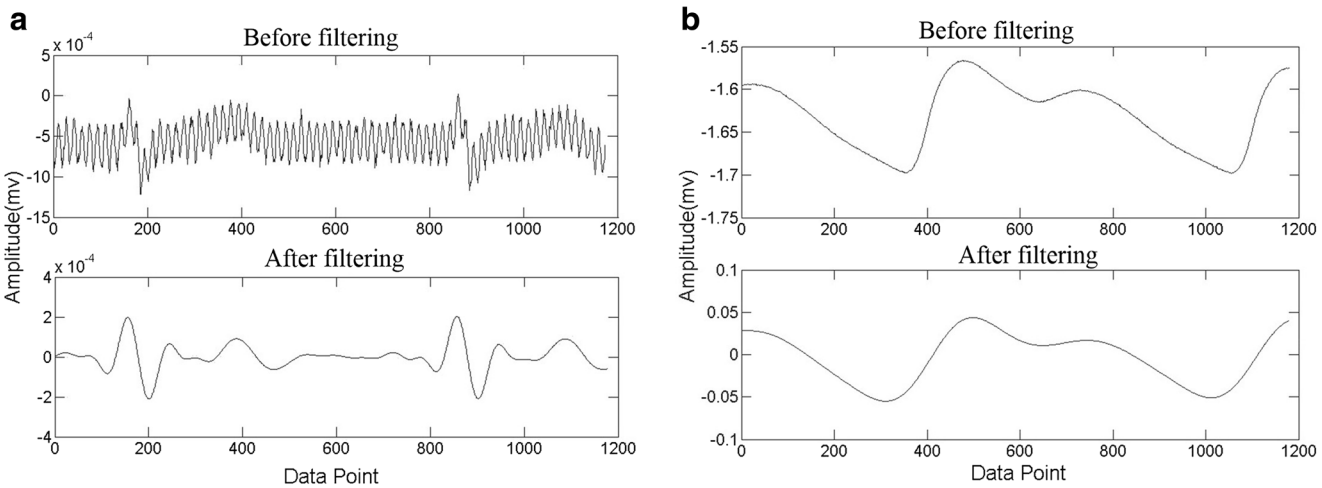

Fig. 7 Signals before and after filtering: **a** ECG and **b** PPG

Table 3 Feature combinations of ECG and PPG signal features

Code	Feature Vector ($x_i =$)
ECG_1	$(\overline{R}_i, R\_sd_i, \overline{RRI}_i, RRI\_sd_i)$
ECG_2	$(\overline{R}_i, R\_sd_i, \overline{RRI}_i, RRI\_sd_i, \overline{PTT}_i, PTT\_sd_i)$
ECG_3	$(cov(R_i, PTT\_sd_i), \overline{R}_i, R\_sd_i, \overline{RRI}_i, RRI\_sd_i)$
ECG_4	$(cov(R_i, PTT\_sd_i), \overline{R}_i, R\_sd_i, \overline{RRI}_i, RRI\_sd_i, \overline{PTT}_i, PTT\_sd_i)$
PPG_1	$(\overline{PPGsys}_i, PPGsys\_sd_i, \overline{PPI}_i, PPI\_sd_i)$
PPG_2	$(\overline{PPGsys}_i, PPGsys\_sd_i, \overline{PPI}_i, PPI\_sd_i, \overline{PTT}_i, PTT\_sd_i)$
PPG_3	$(cov(PPGsys_i, PTT\_sd_i), \overline{PPGsys}_i, PPGsys\_sd_i, \overline{PPI}_i, PPI\_sd_i)$
PPG_4	$(cov(PPGsys_i, PTT\_sd_i), \overline{PPGsys}_i, PPGsys\_sd_i, \overline{PPI}_i, PPI\_sd_i, \overline{PTT}_i, PTT\_sd_i)$

where w^T is the transpose of w and b is the offset of the hyperplane from the origin. This classifier was created based on the training samples, and it was then used to classify new samples. A sample is characterized by a set of features, and the classification essentially involves finding the best boundary (which is formed by $(w^T \cdot x_i + b) = 0$) between the two data classes labeled by y_i.

To find w and b for (4), we must formulate a quadratic optimization problem as follows.

$$\begin{aligned} Minimize\ \ \Phi(w) &= \frac{1}{2}\|w\|^2 = \frac{1}{2}w^T \cdot w \\ \textbf{s.t.}\ \ y_i(w^T \cdot x_i + b) &\geq 1,\ \forall\, i \end{aligned} \tag{5}$$

Because quadratic optimization problems are well-known mathematical programming problems (5), various (nontrivial) algorithms exist that can be applied to obtain the optimal solution for w and b [36]. Suppose that w is a linear combination of a set of support vectors: $w = \sum_{\forall supp\_vector\ i} a_i x_i$, where the set of support vectors is the selection for optimizing the aforementioned optimization problem, and the coefficient a_i is associated with x_i. Notably, (4) describes a linear hyperplane used to separate the two data classes labeled by y_i, and, simultaneously, the acquired signal values of ECG and PPG might be closely adjacent, which hinder linearly separating the two data classes. To address this problem, using kernel mapping functions was proposed to transform x_i to a higher-dimensional space and thereby render the two data classes linearly separable [38]. In this study, a radial-basis kernel function was used to facilitate the classification. Specifically, (6) becomes the new classifier for a new test sample x_j.

$$f(x_j) = \sum_{\forall i} a_i y_i K(x_i, x_j) + b, \tag{6}$$

where $K(x_i, x_j) = e^{\frac{-\|x_i - x_j\|^2}{2\sigma^2}}$, σ is a parameter that must be carefully selected for $K(x_i, x_j)$, x_i is a support vector, and a_i is a coefficient associated with x_i.

4 Results

To conduct the drinking tests, 10 qualified participants were selected from 13 volunteers. The exclusion criteria for selecting participants were based on being heavy drinkers and having a history of cardiovascular problems. The CAGE scale was applied to facilitate the participant screening process. Specific quantities of alcohol were calculated for each participant. Participants were asked to participate in the **cat_A** and **cat_B** experiments during different weeks.

To evaluate the classification performance, precision, recall, accuracy, and F-measure were computed using (7)–(10):

$$Precision = \frac{|TP|}{|TP| + |FP|}, \tag{7}$$

$$Recall = \frac{|TP|}{|TP| + |FN|}, \tag{8}$$

$$Accuracy = \frac{|TP| + |TN|}{|TP| + |TN| + |FP| + |FN|}, \tag{9}$$

$$F = \frac{2 * Precision * Recall}{(Precision + Recall)}, \tag{10}$$

where TP represents a set of test results correctly identified, FP represents a set of test results incorrectly identified, TN represents a set of test results correctly rejected, and FN represents a set of test results incorrectly rejected.

The original design of the proposed system (i.e., the wearable alarm for identification of alcohol intoxication) has three alarm signals: no alarm (NA), mild alarm (MA), and serious alarm (SA). Based on the very strict BrAC limit for driving of 0.15 mg/L reported in [27], the physiological data sets for classification were established according to the three alarm signals, and each data set included the raw signals of ECG, PPG, and BrAC. For NA ($BrAC = 0$ mg/L), no alarm is resulted since the classified physiological data were acquired in a condition without alcohol consumption; for MA ($0 < BrAC < 0.15$ (mg/L)), it was considered to indicate being mildly under the influence of alcohol; and for SA ($BrAC \geq 0.15$ mg/L), it was considered to indicate being intoxicated by alcohol, signifying that vehicle operation should be avoided.

According to the alcohol test procedures in Fig. 3, 240 data sets of raw physiological signals were acquired, including 40 sets for NA, 140 sets for MA, and 60 sets for SA. Through the signal processing procedure depicted in Fig. 5,

the acquired data sets were processed and prepared for the feature combinations shown in Table 3, and we obtained 240 effective feature combinations for the classification of alcohol consumption. To accurately classify the NA, MA, and SA alarms, the application of two SVM classifiers is sufficient to identify either "$BrAC = 0$ mg/L" or "$BrAC \geq 0.15$ mg/L". The SVM classifiers were trained using the feature vectors depicted in Table 3. Because we had eight feature vectors in each feature combination and two SVM classifiers, it was necessary to carry out 16 classifications for each feature combination. Leave-one-out cross-validation was applied on the aforementioned combinations to obtain 16 average results of all combinations, where 8 results are for ECG (Table 4) and 8 for PPG (Table 5). To train the SVM classifiers, an open source machine learning library, Libsvm [39], was employed. The trained SVM classifiers are abbreviated as SVM_{na} and SVM_{sa} for NA and SA, respectively.

Tables 4 and 5 show the classification results obtained by the two classifiers in terms of precision (P), recall (R), and F-measure (F). Table 4 provides the results obtained when using the four ECG feature vectors, whereas Table 5 provides the results obtained when using the four PPG feature vectors. For ECG features in NA, the classified results of SVM_{na} with ECG_3 or ECG_4 were the best (F = 100%), and in SA, SVM_{sa} with ECG_4 the best (F = 96.6%). By observing the features in ECG_3 and ECG_4, we found that the correlation coefficient between an R_i peak and the standard deviation of PTT_i can raise the efficiency of identifying $BrAC = 0$ and $BrAC \geq 0.15$ (mg/L). For PPG features, PPG_3 obtained the best results for SVM_{na} and SVM_{sa} (F = 100 and 92.9(%), respectively). Actually, the correlation coefficient between an R_i (or $PPGsys_i$) peak and PTT_sd_i is beneficial to classify alcohol consumption. By comparing PPG_3 to ECG_3, the $PPGsys_i$ peak is superior to R_i in correlation to PTT_sd_i for identifying alcohol consumption.

In the proposed system, the sequence in which the classifiers are applied to assess alcohol intoxication entails SVM_{na} and then SVM_{sa}. This application sequence is intended to answer the following questions sequentially:

Q1: Does the subject have a blood alcohol level of zero?
Q2: Is the subject over the BrAC limit of 0.15 mg/L?

This multiclassifier arrangement strategy can increase the accuracy of classifying and issuing the NA, MA, and SA alarms according to different BrAC values of alcohol consumption. Because SVM_{na} has the best identification performance with all feature combinations found in Tables 4 and 5, using SVM_{na} first to filter a subject with zero blood alcohol level can reduce the error identification ratio caused by SVM_{sa}. Through the first application SVM_{na}, the positive result of SVM_{na} causes the proposed system to issue an NA alarm signal and assures that $BrAC = 0$ mg/L. If a negative result is obtained, then the system triggers a subsequent test by SVM_{sa}. Basically, it verifies whether $BrAC \geq 0.15$ mg/L. If a positive result is obtained, then an SA alarm signal is provided, and $BrAC \geq 0.15$ mg/L is confirmed; otherwise, the system provides an MA alarm signal and assures that $0 < BrAC < 0.15$ (mg/L).

To give an example for the multiclassifier arrangement, we selected randomly 5 feature combinations from 40 combinations for NA, from 140 combinations for MA, and from 60 combinations for SA, respectively, and it had totally 15 combinations for testing. In Tables 6 and 7, the combinations no.1–5 were selected for testing NA, no.6–10 for testing MA, and no.11–15 for testing SA by applying SVM_{na} and SVM_{sa} simultaneously. The testing results for all feature combinations are listed in Tables 6 and 7, where 60 results are for SVM_{na} and 60 for SVM_{sa} in each table. In the tables, it can be seen that the classification performance of SVM_{na} is perfect. All feature vectors are classified correctly. For SVM_{sa}, there are 6 classification errors happened in each table. In ECG features, SVM_{sa} performed 4 errors for the MA signals and 2 for SA, respectively. In PPG features, it performed 6 errors for MA.

To compute the relative frequency of classification errors for the classifiers, SVM_{na} is zero (or 0%), and SVM_{sa} 6/60 (or 10%) both for ECG and PPG based on the respective

Table 4 Classification results for ECG feature vectors

	ECG_1	ECG_2	ECG_3	ECG_4	(%)
SVM_{na}	97.5	90	100	100	*P*
(BrAC=0)	100	100	100	100	*R*
	98.7	94.7	100	100	*F*
SVM_{sa}	96.4	90.9	96.3	100	*P*
(BrAC≥0.15)	90	87	89.7	93.3	*R*
	93.1	88.9	92.9	96.6	*F*

P: Precision, *R*: Recall, and *F*: F-measure

Table 5 Classification results for PPG feature vectors

	PPG_1	PPG_2	PPG_3	PPG_4	(%)
SVM_{na}	97.5	97.4	100	97.5	*P*
(BrAC=0)	100	100	100	100	*R*
	98.7	98.7	100	98.7	*F*
SVM_{sa}	89.3	96.3	92.9	92.9	*P*
(BrAC≥0.15)	92.6	89.7	92.9	92.9	*R*
	90.9	92.9	92.9	92.9	*F*

P: Precision, *R*: Recall, and *F*: F-measure

Table 6 Classification by the multiclassifier arrangement for ECG feature combinations

No.	ECG_1		ECG_2		ECG_3		ECG_4	
	NA	SA	NA	SA	NA	SA	NA	SA
1	1	0	1	0	1	0	1	0
2	1	0	1	0	1	0	1	0
3	1	0	1	0	1	0	1	0
4	1	0	1	0	1	0	1	0
5	1	0	1	0	1	0	1	0
6	0	1	0	0	0	1	0	0
7	0	1	0	0	0	1	0	0
8	0	0	0	0	0	0	0	0
9	0	0	0	0	0	0	0	0
10	0	0	0	0	0	0	0	0
11	0	1	0	1	0	1	0	1
12	0	1	0	1	0	1	0	1
13	0	1	0	1	0	1	0	1
14	0	1	0	0	0	1	0	1
15	0	1	0	0	0	1	0	1

NA: SVM_{na}, SA: SVM_{sa}; **1** means "Accept", **0** means "Reject"

Table 7 Classification by the multiclassifier arrangement for PPG feature combinations

No.	PPG_1		PPG_2		PPG_3		PPG_4	
	NA	SA	NA	SA	NA	SA	NA	SA
1	1	0	1	0	1	0	1	0
2	1	0	1	0	1	0	1	0
3	1	0	1	0	1	0	1	0
4	1	0	1	0	1	0	1	0
5	1	0	1	0	1	0	1	0
6	0	1	0	1	0	1	0	1
7	0	1	0	0	0	1	0	0
8	0	0	0	0	0	0	0	0
9	0	0	0	0	0	0	0	0
10	0	0	0	0	0	0	0	0
11	0	1	0	1	0	1	0	1
12	0	1	0	1	0	1	0	1
13	0	1	0	1	0	1	0	1
14	0	1	0	1	0	1	0	1
15	0	1	0	1	0	1	0	1

NA: SVM_{na}, SA: SVM_{sa}; **1** means "Accept", **0** means "Reject"

number of the SVM tests. For the application of the multiclassifier arrangement to ECG (or PPG), SVM_{na} can screen out the combinations no.6–15 for the following assessment by SVM_{sa}. However, by applying SVM_{sa} directly to the combinations no.6–15, 6 wrong classification errors would be made as shown in Table 6 (or Table 7). Therefore, we were convinced that the multiclassifier arrangement may confine the possible classification errors to raise the classification efficiency.

To compare the performance of this work with a previous work [18], Table 8 shows the various aspects of comparing the two works. In [18], the experimental procedure was based on the work-flow of recording normal ECG signals for 2 min., alcohol intake, 1-hour rest for alcohol absorption to reach $BAC > 0.02$ g/dL, recording alcoholic ECG signals for 2 min., and repeating the above procedure 3 times on 3 different days. Thus, there are 2 min. for normal and another 2 min. for alcoholic ECG signals recorded from 50 participants on 3 days, which is totally 600 min. ECG signals being recorded. The recorded ECG samples were categorized into two classes, normal ($BAC = 0$ g/dL) and drunk (identified by 10 key features [18]). In addition, participants were asked to stay stationary to avoid motion artifacts to ECG signal.

In this work, the above means were practiced in a similar way, except that we had the BrAC values recorded, $BAC > 0.04$ g/dL, 15 min. rest for alcohol absorption, 7 min. rest after 3 min. ECG recording under drinking, 17 selected features for drunk classification, and 3 categories of ECG samples, i.e., NA, MA, and SA. In addition, we implemented the alcohol test procedure in two drinking experiments, **cat_A** and **cat_B**, on 2 different days. As mentioned earlier, there are 240 data sets of 3 min. raw signals being recorded, which equal to 720 min. ECG signals.

In [18], the ECG signal acquisition means adopted the precordial chest leads, which are not easy to be integrated with smart and wearable devices. On the contrary, the proposed system adopted the standard limb lead 1, which is easier to be applied to the devices. Especially, PPG was adopted in the system to increase the DUI classification efficiency and is easier to be integrated with the devices due to using one single skin contact. In Table 8, the accuracy disclosed in [18] is about 88%; the accuracy disclosed in this study is about 95%, which is obtained by averaging the test results performed by SVM_{na} and SVM_{sa}. The reasons for better results in this study are due to the higher BAC level, which makes ECG and PPG features variate more prominently for DUI classification, and the incorporation of PPG signals increasing the classification efficiency.

In summary, the classification performance of the proposed system, based on the two SVMs and the eight ECG and PPG combinations, is adequate to help preventing DUI, while remaining compatible with the requirements imposed by wearable devices. In the proposed system, the

Table 8 Comparison of this work with a previous work [18]

Aspects	Previous work [18]	This work
Experimental procedure	One process repeated 3 times on 3 different days	Two processes on 2 different days
BAC level	>0.02 g/dL	> 0.04 g/dL
Classes being classified	Normal/drunk	NA/MA/SA
Total ECG signal time (min.)	600	720
Defined features	10	17
ECG acquisition	Precordial chest leads	Standard limb lead 1
Convenience in wearing	ECG chest leads—*bad*	ECG limb lead 1—*average*; PPG—*good*
Accuracy (9)	88%	95%

selection of efficient features, which are used to build the feature combinations, for alcohol consumption identification is quite important. In particular, the configuration used for acquiring the signals is characterized by reduced complexity, but at the same time it preserves the quality of classification. Therefore, the features (Table 2) are specifically selected for wearable devices. The features used in the system are based on heart rates, the peak values of ECG QRS waves and PPG systole waves, and a few time domain intervals [18, 32]. The classification results in Tables 4 and 5 confirmed that excessive alcohol consumption may produce prominent changes in heart rates and the peak values of cardiac waves, and the best feature vectors for ECG and PPG are ECG_4 and PPG_3, respectively. Since the acquisition convenience of PPG signals, where a single point of skin contact is needed, is much better than ECG, where at least two contact points are required, we suggest that the technological configuration using PPG with the PPG_3 feature vector is preferable for smart and wearable devices than with ECG. Actually, in terms of medical equipment, acquiring the PPG signals is simpler than the acquisition of ECG waves and blood alcohol content. Finally, we found that the alcoholic PPG signals (Tables 3, 4, and 5) in the alcohol consumption identification are almost as effective as ECG.

5 Conclusion

Due to technological advancement, the smart and wearable sensing devices offer a promising solution for DUI prevention. In [5–8], the physiological signals of RRI and HRV have been shown to be affected significantly by alcohol consumption. However, these studies cannot be applied to DUI prevention due to the lack of feasible signal extraction and classification mechanisms for the devices. In [18], which the authors state is the first study of its kind, four SVM-based classifiers with various kernel functions were proposed, with the highest accuracy of 88%. However, their signal acquisition method is very inconvenient to be applied to the devices.

In this study, we propose a simple and accurate scheme based on SVM for facilitating the identification of alcohol intoxication. Two SVM classifiers were devised to identify whether $BrAC = 0$ mg/L or $BrAC \geq 0.15$ mg/L (i.e., the aforementioned questions Q1 and Q2). According to the tested results, the system provides an alarm of NA, MA, or SA. In addition, the system was tested based on the four ECG feature vectors and the other four PPG vectors, thereby enabling the advantages of various technological configurations to be compared for developing smart and wearable DUI prevention devices. In terms of the F-measure in Tables 4 and 5, the system performance achieved 95% on average.

The performance evaluation indicates that the technological configuration using PPG with PPG_3 is preferable for developing a portable or wearable DUI prevention device. This is because the PPG signal acquisition with only one contact point is sufficient. In the future, we plan to investigate whether the results of the proposed method are affected by other factors, such as emotions.

Acknowledgements The authors thank the National Science Council, Taiwan, for supporting this study under the contract NSC 100-2218-E-224-008-MY3, and the participants who assisted in the experiment.

References

1. Borkenstein R, Zylman R, Ziel W, Shumate R, Crowther R (1974) The role of the drinking driver in traffic accidents (the grand rapids study), 2nd edn. Indiana Univ., Center for Studies in Law in Action, Department of Forensic Studies. https://books.google.com.tw/books?id=mSARngEACAAJ
2. Global status report on road safety (2015). http://www.who.int/violence_injury_prevention/road_safety_status/2015/en/
3. Sweedler BM, Biecheler M-B, Laurell H, Kroj G, Lerner M, Mathijssen M, Mayhew D, Tunbridge R (2004) Worldwide trends in alcohol and drug impaired driving. Traffic Inj Prev 5(3):175–184

4. WHO et al (2007) Drinking and driving: a road safety manual for decision-makers and practitioners. Global Road Safety Partnership c/o International Federation of Red Cross and Red Crescent Societies
5. Malpas SC, Whiteside EA, Maling TJB (1991) Heart rate variability and cardiac autonomic function in men with chronic alcohol dependence. British Heart J 65(2):84–88
6. Koskinen P, Virolainen J, Kupari M (1994) Acute alcohol intake decreases short-term heart rate variability in healthy subjects. Clin Sci 87(2):225–230
7. Ryan J, Howes L (2002) Relations between alcohol consumption, heart rate, and heart rate variability in men. Heart 88(6):641–642
8. Bau PF, Moraes RS, Bau CH, Ferlin EL, Rosito GA, Fuchs FD (2011) Acute ingestion of alcohol and cardiac autonomic modulation in healthy volunteers. Alcohol 45(2):123–129
9. Carpeggiani C, Emdin M, Macerata A, Raciti M, Zanchi M, Bianchini S, Kraft G, Abbate A (2000) Heart rate variability modified by altitude exposure. In: Computers in cardiology 2000. IEEE, pp 817–820
10. Carpeggiani C, Erndin M, Macerata A, Raciti M, Zanchi M, Bianchini S, Abbate A (2001) Altitude distress influence on cardiac function. In: Computers in cardiology 2001. IEEE, pp 325–328
11. Alsafwah S (2001) Electrocardiographic changes in hypothermia. Heart & Lung: J Acute Crit Care 30(2):161–163
12. Graham CA, McNaughton GW, Wyatt JP (2001) The electrocardiogram in hypothermia. Wilderness Environ Med 12(4):232–235
13. Simoons M, Hugenholtz P (1975) Gradual changes of ecg waveform during and after exercise in normal subjects. Circulation 52(4):570–577
14. Cai J, Liu G, Hao M (2009) The research on emotion recognition from ecg signal. In: International conference on information technology and computer science, 2009 (ITCS 2009), vol 1. IEEE, pp 497–500
15. Xianhai G (2011) Study of emotion recognition based on electrocardiogram and rbf neural network. Procedia Eng 15:2408–2412
16. Karlen W, Mattiussi C, Floreano D (2009) Sleep and wake classification with ecg and respiratory effort signals. IEEE Trans Biomed Circ Syst 3(2):71–78
17. Allen J (2007) Photoplethysmography and its application in clinical physiological measurement. Physiol Measur 28(3):R1. http://stacks.iop.org/0967-3334/28/i=3/a=R01
18. Wu CK, Tsang KF, Chi HR, Hung FH (2016) A precise drunk driving detection using weighted kernel based on electrocardiogram. Sensors 16(5):659. http://www.mdpi.com/1424-8220/16/5/659
19. Intoximeters Alco-SensorIV Intoximeters
20. ADInstruments, Gp amp owner's guide (2008). http://cdn.adinstruments.com/adi-web/manuals/GP_Amp_OG.pdf
21. ADInstruments, Bio amp owner's guide (2009). http://cdn.adinstruments.com/adi-web/manuals/Bio_Amp_OG.pdf
22. ADInstruments, Powerlab /30 series owner's guide (2009). http://cdn.adinstruments.com/adi-web/manuals/PowerLab_30_Series_OG.pdf
23. Page R (2005) Twelve-lead ECG for acute and critical care providers, EKG Series. Pearson Prentice Hall. https://books.google.com.tw/books?id=TOxLAQAAIAAJ
24. Friesen GM, Jannett TC, Jadallah MA, Yates SL, Quint SR, Nagle HT (1990) A comparison of the noise sensitivity of nine qrs detection algorithms. IEEE Trans Biomed Eng 37(1):85–98
25. Electronics Hub (2015) Butterworth filter Available at http://www.electronicshub.org/butterworth-filter/
26. Lee H, Lee J, Jung W, Lee G-K (2007) The periodic moving average filter for removing motion artifacts from ppg signals. Int J Control Autom Syst 5(6):701–706
27. Warner A (1998) Drug abuse handbook. Clin Chem 44(7):1586–1586. http://clinchem.aaccjnls.org/content/44/7/1586.full.pdf
28. Stöckl D, Dewitte K, Thienpont LM (1998) Validity of linear regression in method comparison studies: is it limited by the statistical model or the quality of the analytical input data? Clin Chem 44(11):2340–2346. http://clinchem.aaccjnls.org/content/44/11/2340.full.pdf
29. Jones AW The relationship between blood alcohol concentration (BAC) and breath alcohol concentration (BrAC): a review of the evidence, Road Safety Web Publication 15
30. Searle J (2015) Alcohol calculations and their uncertainty. Med Sci Law 55(1):58–64. pMID: 24644224. doi:10.1177/0025802414524385
31. Allen J, Columbus M (1997) Assessing alcohol problems: a guide for clinicians and researchers, NIAAA treatment handbook series 4, Diane Pub. https://books.google.com.tw/books?id=0xReiqa4WzUC
32. Sereny G (1971) Effects of alcohol on the electrocardiogram. Circulation 44:558–564. doi:10.1161/01.CIR.44.4.558
33. He X, Goubran RA, Liu XP (2013) Evaluation of the correlation between blood pressure and pulse transit time. In: IEEE International symposium on medical measurements and applications proceedings (MeMeA 2013). IEEE, pp 17–20
34. Li C, Zheng C, Tai C (1995) Detection of ecg characteristic points using wavelet transforms. IEEE Trans Biomed Eng 45:21–28
35. Legarreta IR, Addison PS, Reed MJ, Grubb N, Clegg GR, Robertson CE, Watson JN (2005) Continuous wavelet transform modulus maxima analysis of the electrocardiogram: beat characterisation and beat-to-beat measurement. Int J Wavelets, Multiresolution Inf Process 03(01):19–42. doi:10.1142/S0219691305000774
36. Chavan MS, Agarwala R, Uplane M (2006) Use of kaiser window for ecg processing. In: Proceedings of the 5th WSEAS international conference on signal processing, robotics and automation. World Scientific and Engineering Academy and Society (WSEAS), pp 285–289
37. Cubbon RM, Ruff N, Groves D, Eleuteri A, Denby C, Kearney L, Ali N, Walker AMN, Jamil H, Gierula J, Gale CP, Batin PD, Nolan J, Shah AM, Fox KAA, Sapsford RJ, Witte KK, Kearney MT (2016) Ambulatory heart rate range predicts mode-specific mortality and hospitalisation in chronic heart failure. Heart 102(3):223–229
38. Cortes C, Vapnik V (1995) Support-vector networks. Mach Learn 20(3):273–297
39. Chang C-C, Lin C-J (2011) Libsvm: a library for support vector machines. ACM Trans Intell Syst Technol (TIST) 2(3):27:1–27:27